Res. Rep. Fac. Eng. Mie. Univ. Vol.2, pp.1 -9 (1977)

Original Paper

Water Flow in a Horizontal Pipe with Internal Spiral Ribs

Sadao KUZUHARA, Toshihiko SHAKOUCHI and Koichi SUGINO
(Department of Mechanical Engineering)

(Received September 15, 1977)

This report dicusses the loss of head and axial or peripheral velocity distribution when water was made to flow through a horizontal pipe with two spiral ribs on its internal wall. Helical angle of the rib was 10° or 30°, and internal diameter of the rib was one or two inches.

Results obtained were as follows;

(1) Flow loss of head increased with increase of helical angle and sectional angle of the rib. From the viewpoint of the characteristic of the flow loss, the ribbed pipe was between a smooth pipe and a rough one.

(2) Intensity of rotation of the flow increased with increase of helical angle of the rib, but flow loss failed to grow to that extent.

(3) Axial velocity distribution showed fairly good agreement with that of rough pipe to a certain relative roughness, but velocity near the pipe wall was larger to some degree than in the case of rough pipe.

1. Introduction

When transport of a large volume of solid particles with small friction loss of head through a horizontal pipe is required, it is advisable to use relatively low velocity of flow and large concentration of particles. But this tends to settle the particles and consequently leads to pipe blockage.

To solve this problem, it is thought that some method of causing forced and continuous turbulence in the pipe might provide buoyant force to solid particles and keep them from deposition.

Charles et al.[1),2)] have experimented with this concept, using special pipes with an internal spiral rib and fine or coarse sand.

The authors carried out some fundamental experiments, as a first step in this approach, using water flow in several pipes with two internal spiral ribs. In such a case of single phase flow, Charles et al. have reported on the velocity

distribution of air flow through a 2-inch pipe with a single rib, indicating that a strong rotating flow exists near the rib.

2. Nomenclature

D : internal diameter of pipe
D′ : shown in Fig. 1
g : acceleration of gravity
h : height of rib
h_ℓ : loss of head
i : hydraulic gradient
i_0 : hydraulic gradient of smooth pipe
L : length of test section
m : = D/h
p : pitch of rib
Re : Reynolds number (= VD/ν)
r : radius of pipe
V : mean velocity of flow
v : velocity of flow at radius r
v_t : peripheral velocity component of flow at radius r
v_z : axial velocity component of flow at radius r
v_{zm} : maximum axial velocity at the center of pipe
v_* : frictional velocity
y : co-ordinate perpendicular to axis of pipe
Z : number of ribs
ε : roughness of pipe wall
θ : = $90° - \phi$
λ : coefficient of loss of head for the ribbed pipe
λ_B : = $0.3164\ Re^{-\frac{1}{4}}$ (coefficient by Blasius)
ν : kinematic viscosity
ρ : density
τ : frictional stress
ϕ : helical angle of rib

3. Pipes used

As shown in Fig. 1, the pipes used had two internal spiral ribs ("ribbed pipe" hereafter) of which helical angle was 10° and 30°, and the nominal diameter was 1- or 2-inch. Cross section of the pipe are shown in Fig. 1-⑤, ⑥. Shapes of the rib were round and two heights

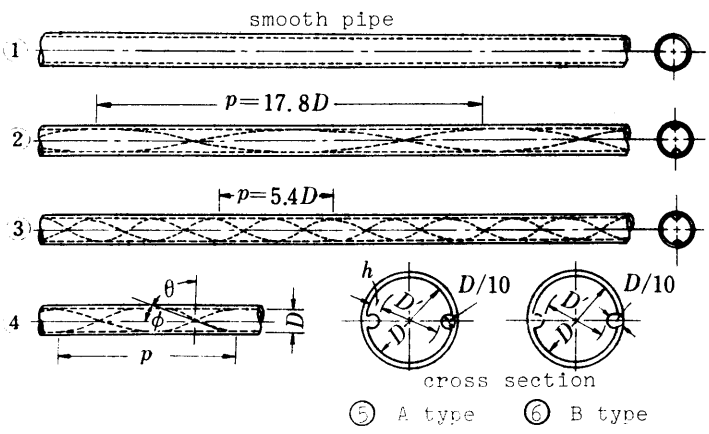

Fig. 1 Pipes used

were used; relatively high ("A type" hereafter) and low ("B type" hereafter). B type was used for 2-inch pipe only. Ordinary pipe without ribs ("smooth pipe" hereafter) was also used in order to get a basis for comparison with ribbed pipes. Ribbed pipes and smooth pipes were both transparent vinyl chloride types of facilitate visual observation of the flow.

pipe symbol	D mm	z	ϕ deg	θ deg	p/D	d mm	$h=\frac{D-d}{2}$	$m=\frac{D}{h}$
100	25.0	0	—	—	∞	—	0	∞
200	50.8							
121A	26.5	2	10	80	17.8	21.5	2.5	10.6
221A	51.7					41.7	5.0	10.3
221B	50.1					42.8	3.7	13.5
123A	27.0	2	30	60	5.4	22.0	2.5	10.8
223A	50.6					40.6	5.0	10.1
223B	51.9					44.9	3.7	14.8

Table 1 Dimensions of pipes used

Table 1 shows pipe dimensions referring to the symbols written in Fig. 1. With reference to the pipe symbols, the hundredth rank of numbers shows the nominal diameter of the pipe, the tenth rank shows the numbers of the ribs, and the first rank shows the helical angle of the rib. In the table, $p/D = \infty$ does not mean the ribs parallel to the axis of the pipe but the smooth pipe.

4. Experimental apparatus and procedure

4. 1 Measurement of head loss

Figure 2 illustrates the apparatus. The test section was about 8.0 m long. Flow corrector and sufficient length of smooth pipe were used to ensure fully developed flow in the test section. Head tank or pump was used to feed water in the region of relatively low or high velocity respectively. Pressure taps were equipped at 10 points as shown in Fig. 2 and pressure loss between them was measured by water column manometers. Since pressure taps were equipped midway between the ribs and pressure losses were measured in the region of fully developed flow in the test section, the effect of ribs and centrifugal force caused by rotation was avoided. Experiments covered the range of Re = (0.9 ~ 1.2) x 10^4.

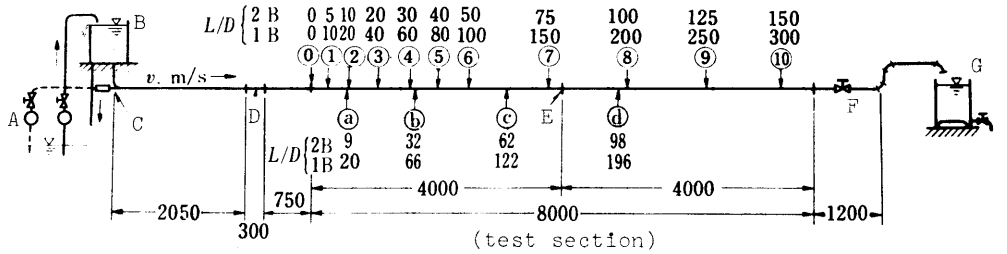

⓪~⑩ : positions of pressure taps
ⓐ~ⓑ : positions of velocity measurements
A : pump, B : head tank, C : electro-magnetic flow meter, D : honeycomb, E : coupler, F : valve, G : measuring tank

Fig. 2 Experimental apparatus

4. 2 Measurement of velocity distribution

Velocity distribution of about three kinds of mean velocity (0.8, 2.0 and 3.3 m/s) was measured at the four sections (ⓐ, ⓑ, ⓒ and ⓓ in Fig. 2) of 221A and 223A pipes. Direction and magnitude of velocity were measured by the use of a previously checked cylindrical tube, traversing it vertically along the diameter of the test pipe. Diameter of the tube was 3.2 mm and had three radial holes. Flow rate was measured by an electromagnetic flowmeter set in series in this line. Experiments covered the range of $Re = (0.9 \sim 13.5) \times 10^4$. Static and dynamic pressure were measured by mercury column manometer at high velocity and carbon tetrachloride column manometer at low velocity respectively. A cathetometer was used to read the manometer.

5. Experimental results and considerations

5. 1 Hydraulic gradient

Figures 4 and 5 show the relations of the loss of head per unit length of the pipeline, namely the hydraulic gradient i vs. mean velocity V of water flow for 1- and 2-inch pipe respectively. The straight lines i in figures mean the losses calculated from λ_B, and λ_B gives the coefficient of loss of head calculated from Blasius equation for turbulent flow in a ordinary smooth pipe (Nomenclature and Fig. 8). Experimental results for smooth pipe almost agree with this calculated straight line. The loss of head for ribbed pipe is larger than that for smooth pipe, and furthermore that for $\phi = 30°$ shows a large loss. However, they are approximately parallel to the calculated straight line. In addition to that, "A type" apparently shows a large loss compared to "B type" in 2-inch pipe. When the relations between V and i in Figures 4 and 5 are shown by the equation

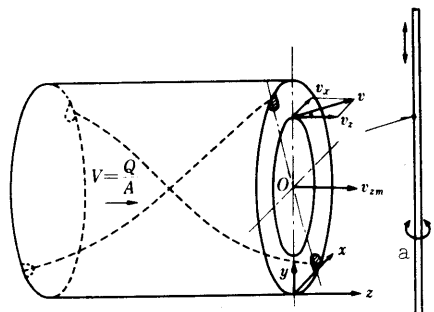

a : three-hole pitot-tube

Fig. 3 Co-ordinate and velocity

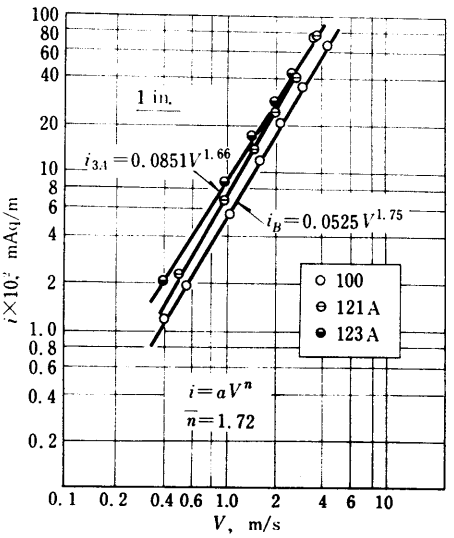

Fig. 4 Loss of head (1" pipe)

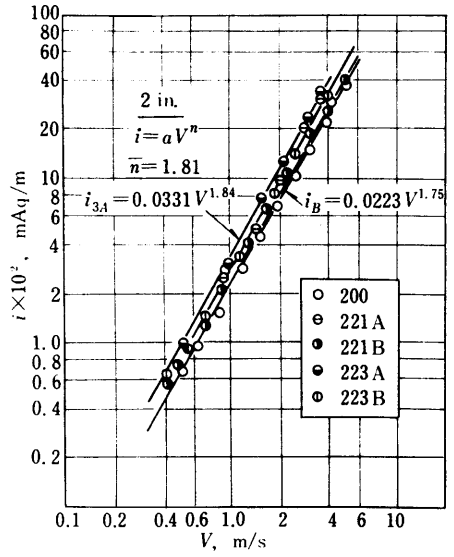

Fig. 5 Loss of head (2" pipe)

$i = aV^n$ (1),

the value of "a" and "n" are obtained as shown in figures for example. Table 2 shows these values for all pipes tested. The mean value of "n" is n = 1.7 for 1-inch pipe and n = 1.8 for 2-inch pipe.

	pipe	i	a	n	$\bar{n}$
1 B	smooth	i_B	0.0525	1.75	1.72
	100	i_o	0.0511	1.77	
	121A	i_{1A}	0.0676	1.74	
	123A	i_{3A}	0.0851	1.66	
2 B	smooth	i_B	0.0223	1.75	1.81
	200	i_o	0.0205	1.79	
	221A	i_{1A}	0.0269	1.86	
	223A	i_{3A}	0.0331	1.84	
	221B	i_{1B}	0.0244	1.81	
	223B	i_{3B}	0.0268	1.78	

Table 2 Values of "a" and "n" in eq. (1)

5. 2 p/D and head loss increase rate

As shown above, the loss of head for an ordinary smooth pipe at turbulent flow showed little difference from that for the pipe without ribs, and the value of "n" in eq. (1) for ribbed pipe, namely, the gradient of the straight lines in Fig. 4 and 5, was almost equal over the range of Reynolds number in this experiment as shown in table 2. Therefore, we can compare the head loss on the basis of the smooth pipe and by means of comparison of "a" in eq. (1). Figure 6 shows the relations between p/D and $i/i_o = a$, where $i = i_{1A}$, i_{3A}, i_{1B}, i_{3B} and the effect of the helical angle of the rib. We can see that i/i_o of "A type" does not depend upon the pipe diameter but on the helical angle of the rib. On the other hand, i/i_o of "B type" may also be expressed by one curved line for 1- and 2-inch pipe, though 2-inch pipe was only employed in this case. In the case of $\phi = 30°$, it can be said that the head loss of section A or B type becomes 1.22 or 1.09 times that of $\phi = 10°$ respectively. In either case, both of the curved lines approach the value of unity when p/D increases towards infinity.

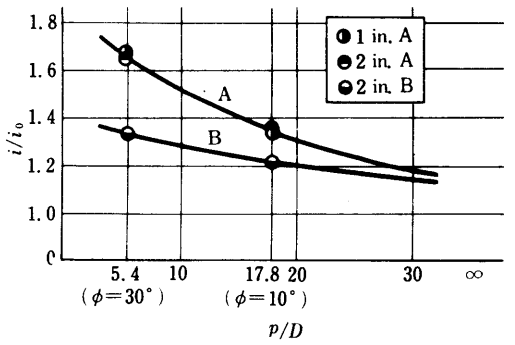

Fig. 6 Head loss increase rate

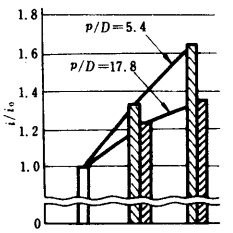

smooth, B type, A type

Fig. 7 Head loss increase rate

5. 3 Shapes of pipe cross section and head loss increase rate

As shown in Fig. 6, there are clear differences between the loss of head ratio i/i_o for both types A and B. We can easily imagine that the flow loss along the pipe of section A type is larger than that for section B type because the rib of the former is higher than that of the latter. Figure 6 shows this relation quantitatively. Figure 7 is an another expression of the relations between the shape of section and head loss ratio i/i_o. From this figure, it can be seen that the head loss ratio for section A type is 1.10 times as large as that for section B type at p/D = 5.4 (ϕ = 30°).

5. 4 Coefficient of loss of head

Water flow in a ribbed pipe consists of two flows; one is an overflow beyond the rib and another is a rotating flow. Therefore, it is conceivable that the loss of head for the ribbed pipe fails to depend upon the friction between fluid and pipe wall only. Now, expressing the loss of head by the next equation as for turbulent flow in a smooth pipe

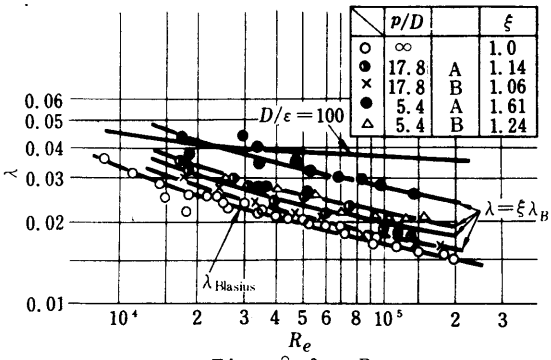

Fig. 8 λ - Re

$$h_\ell = \lambda \frac{\ell}{D} \frac{V^2}{2g} \qquad (2),$$

we obtain the relation between λ and Re as shown in the figure. And we can see that coefficient λ depends on p/D and the shape of the cross section, regardless of diameter, and it is expressed by curved lines parallel to that of λ_B. Ribbed pipe tends to be between smooth pipe and rough pipe with a large pitch wavy surface in regards to the coefficient. Then λ is quantitatively expressed as follows.

$$\lambda = \xi \lambda_B \qquad (3)$$

Approximate values of ξ and, for reference, λ for a surface of relative roughness $D/\varepsilon = 100$ are written in Fig. 8.

5. 5 Velocity distribution (peripheral velocity component)

Velocity distributions measured in the case of relatively low, middle and high velocity for 221A and 223A pipes are shown in Fig. 9, where v_x, v_z and v are peripheral or axial velocity component and mean velocity respectively. The indications a-a, b-b, c-c and d-d show the position of ribs in the cross section where velocity distributions were measured. At measuring ⓐ (L/D = 9 in Fig. 2), v is small and it can be said that the flow is not yet fully developed. At ⓑ (L/D = 32), ⓒ (L/D = 62) and ⓓ (L/D = 98), the profile of velocity distributions v_x/V and v_z/V for each pipe diameter and each velocity resembles each other in shapes, and peripheral velocity components become smaller near the center of the pipe. Peripheral velocity components v_x for 223 pipe of $\phi = 30°$ is larger than that for 221 pipe of $\phi = 10°$. This shows that the circulating flow for $\phi = 30°$ is more intensified than for $\phi = 10°$. Velocity distributions near the pipe wall near the rib do not markedly differ from those distant from the rib. Charles et al. have measured the velocity distributions of air flow at 60 points for 2-inch pipe with a 1/4-inch x 1/4-inch continuous spiral rib of p/D = 3.0. Flow rate of air was 50.2 ft^3/min., but the results failed to show a distinct difference between the velocity distributions near the rib and distant from it. Now, we assume that the areas F_1 and F_3 shown in Fig. 9 express the intensity of rotating flow. The intensity of the rotating flow for 223A pipe is about twice that for 221A pipe at the positions ⓑ, ⓒ and ⓓ where the flow attains the fully developed state at each mean velocity.

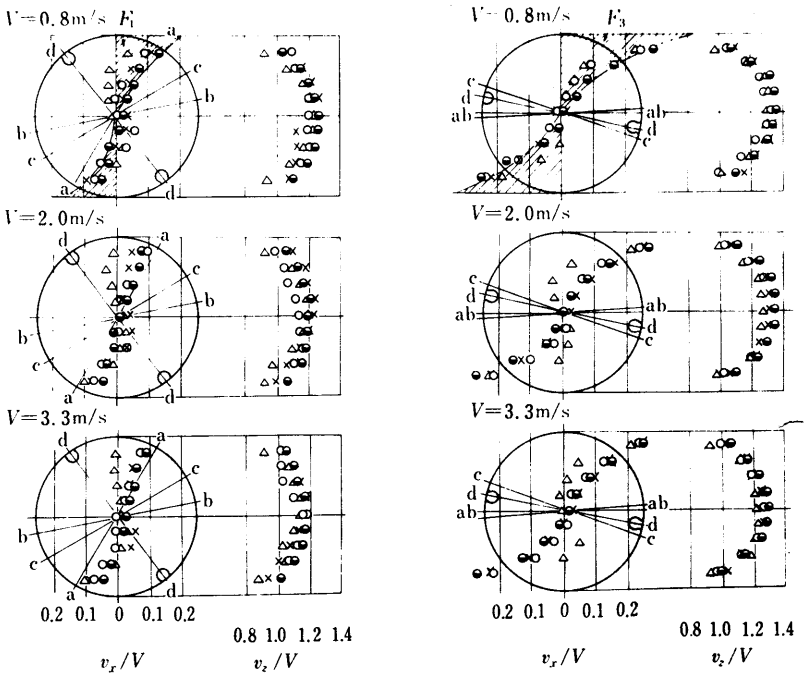

(I) 221A pipe (II) 223A pipe

△; a, ○; b, ×; c, ⊖; d : positions of velocity measurement in Fig. 2

Fig. 9 Peripheral velocity distribution

Though the result for 221A pipe showed a little scatter, this may be affected by the direction of the rib at the test section.

5. 6 Velocity distribution (axial velocity component)

Figure 10 shows the axial velocity distributions with no dimension for various mean velocities, where

$$v_* = \left(\frac{\tau_0}{\rho}\right)^{\frac{1}{2}} = v_{zm}\left(\frac{\lambda}{8}\right)^{\frac{1}{2}} \qquad (4).$$

Axial velocity distributions for smooth and rough pipes are shown by solid lines in the figure for reference. For mean velocities of 0.8, 2.0 and 3.3 m/s, velocity distributions of 221A pipe are equivalent to those of rough pipe with a relative roughness 90, 200 and 350, and those of 223A pipe to 30, 60 and 90, respectively. Axial velocity distributions for 223A pipe with large helical angle of ribs are equivalent to those for a rough pipe with large roughness at every mean velocity. In either case, axial velocity distributions are equivalent to those of large roughness as the mean velocity increases. Figure 11 shows the relations between $(v_{zm} - v_z)/v_*$ and y/r for 221A and 223A pipe. The solid line denotes the velocity distribution for rough pipe, and by way of example, the calculated results for v = 3.3 m/s are also plotted. It is obvious from Fig. 11 that the axial velocity distributions can be expressed fairly well

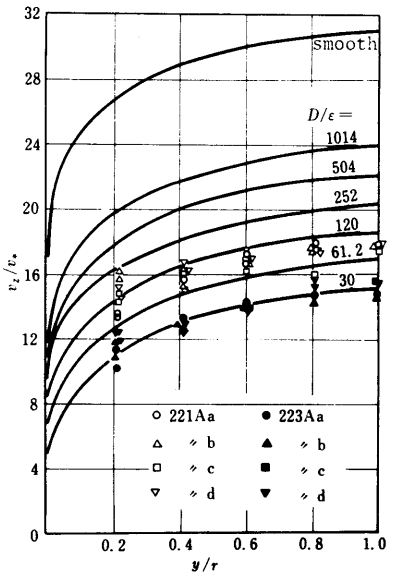

Fig. 10-1 V = 0.8 m/s

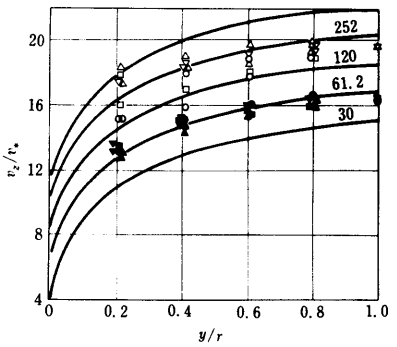

Fig. 10-2 V = 2.0 m/s

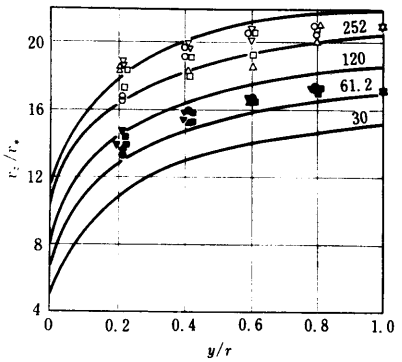

Fig. 10-3 V = 3.3 m/s

Fig. 10 Axial velocity distribution

by those for rough pipe,but they are flatter than those for the latter; in other words, the axial velocities near the pipe wall are larger than expected. This is attributed to the rather large peripheral velocity caused by ribs.

6. Relation between strength of rotating flow and loss of head

The relation between the strength of rotating flow defined by the area F_1 and F_3 in section 5. 5 and the loss of head for 221 A and 223A pipe, is shown in Fig. 12. The strength of rotating flow for ϕ = 30° is double that for ϕ = 10°, and large agitating effects are expected. But it does not always follow that the loss of head for ϕ = 30° dou-

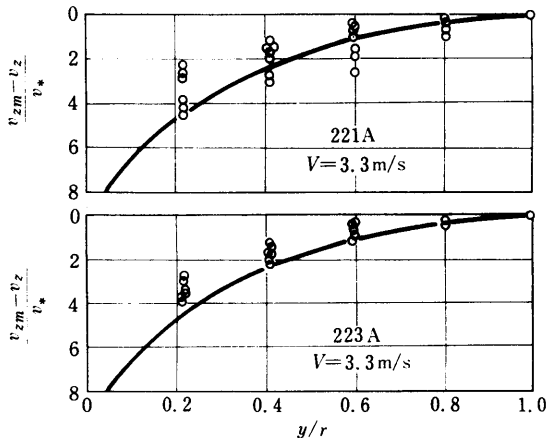

Fig. 11 Axial velocity distribution

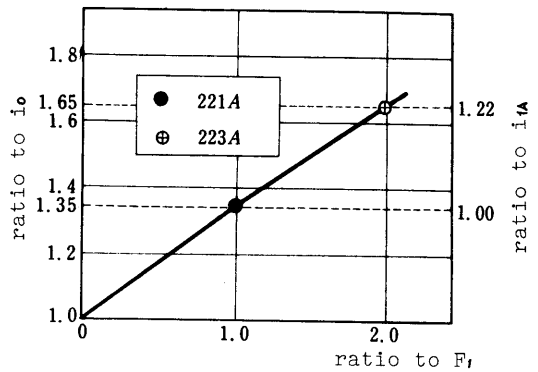

Fig. 12 Relation between strength of rotating flow and increase of flow resistance

ble that for $\phi = 10°$ because it is about 1.35 times for smooth pipe and 1.22 times for ribbed pipe of $\phi = 10°$ respectively.

7. Conclusions

From an experiment of water flow through a special pipe with two internal spiral ribs the following conclusions were obtained.

(1) The flow resistance of water through the ribbed pipe became larger as the area of cross section and the helical angle of ribs increased. In regard to the loss of head, ribbed pipe showed a intermediate property between smooth pipe and rough one.

(2) Both the strength of rotating flow and the loss of head increased with the angle of the ribs, but the rate of head loss increase was less than that of rotating flow intensity.

(3) Axial velocity distribution could be expressed fairly well for a pipe with a certain roughness, but it was flatter than for an ordinary rough pipe, namely, the axial velocities near the pipe wall were larger than expected.

Acknowledgments

The authors wish to express their thanks to Prof. M.E. Charles who kindly sent us reprints of his paper, and to Toa Gosei Kagaku Kogyo Co. which provided us with the special pipes used in this experiment.

References

(1) M.E. Charles: Proc. of Hydrotransport 1, BHRA (1970)
(2) M.E. Charles: Canad. J. Chem. Eng., 49 (1971)